Simulation and Processing Techniques of Surface Electromyography Signal to Control a Lower Extremity Exoskeleton

Ngoc-Khoat Nguyen and Thi Mai Phuong Dao

Abstract — In recent years, surface electromyography (sEMG) signals which reflect directly human muscle activity have played a significant role in control of a lower extremity exoskeleton system. Our study concentrates on simulation and processing techniques of sEMG signal that we are applying to our exoskeleton robot. Simulation and experiment results are presented and analyzed deeply to validate the techniques mentioned. These results are being applied in our ongoing design of a lower extremity exoskeleton system which is used to assist a soldier to walk with or without load carrying.

Index Terms— Lower extremity exoskeleton, Model, sEMG, Simulation, Processing, Technique, Wavelet transform

1 Introduction

SURFACE electromyography signal – based control is one of the successful and efficient control methods for a lower extremity exoskeleton robot. Many researchers have been considering deeply this technique. Most of them attempted sEMG signal which directly reflects human muscle activity as one of the most important control signals for their systems [7], [8], [10], [11]. Raw sEMG signals which are recorded by surface electrodes, however, are not being used by many researches because of certain drawbacks, such as very small and stochastic amplitude, unstable shape, and many noises [12]. Although sEMG signals can be measured carefully, their artifacts often occur to destroy and make them almost useless. As a result, it is necessary to process these raw signals to create significant control signals by applying sEMG processing techniques [1], [2], [12].

For the start point of this work, the first phase of this paper introduces three techniques to simulate sEMG signal. These techniques are based on three sEMG models: random variable model, layer volume conduction model, and fiber action potential model. Simulation results of these models are obtained by using MatLab software. Three of these results illustrate clearly sEMG signals of Gastrocnemius Medialis, Tibialis Anterior, and Soleus muscles during human gait cycle which will significantly impact on our ongoing design of a lower extremity exoskeleton system.

In the second phase, a sEMG signal processing technique will be considered. Continuous wavelet transform (CWT) is used efficiently to analyze and remove noises from the raw sEMG signal which has many drawbacks as mentioned above. In order to generate control signals such as forces [7], [14], [16] in accordance with sEMG signals, a sEMG-to-force relationship is given. Results of this processing technique are analyzed by both simulation and experiment during human gait cycle.

2 Simulation Techniques for SEMG Signal

SEMG simulation techniques are very plentiful and they depend on actual aims. For simple goals, sEMG signal can be simulated as a random distribution [17]. To yield this work, a pseudo – Gaussian distribution with the roughly equal mean of zero is used. Fig. 1 presents the graph of sEMG which is plotted as a pseudo – Gaussian distribution. This simulation technique is also used to analyze the power spectrum density (PSD) of sEMG signal.

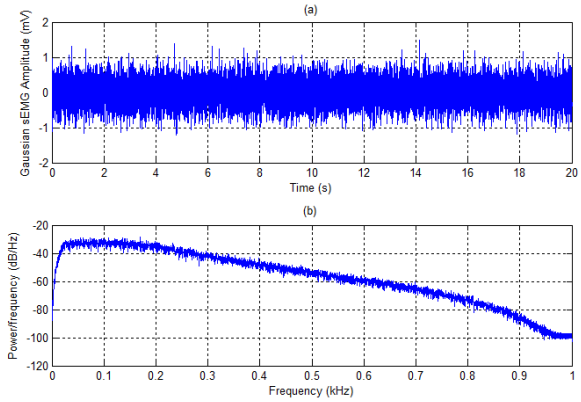

Fig. 1. Simulation of the Gaussian sEMG signal
(a) Shape of the Gaussian sEMG signal
(b) Power Spectrum Density of the Gaussian sEMG signal

In order to understand the relationship between physiological and electrical models, a layer volume conduction model is used as shown in Fig. 2. According to this model, three layers of a physiological model (skin, fat tissue, and muscle fiber layer) are substituted by components of an electrical model. Values of resistors and capacitors are computed by [13], [20] to simulate sEMG signal.

- *Ngoc-Khoat Nguyen is currently pursuing PhD degree program in automation in University of Electronic Science and Technology of China, China. At present, he is also a lecturer in Electricity Power University, Hanoi, Vietnam. Phone-+8613088051248. E-mail: khoatnn@epu.edu.vn*
- *Thi Mai Phuong Dao is currently pursuing PhD degree program in Automation in Hunan University, China. At present, she is also a lecturer in Hanoi University of Industry, Hanoi, Vietnam. Phone - +8615200931744. E-mail: bkblackrose@yahoo.com*

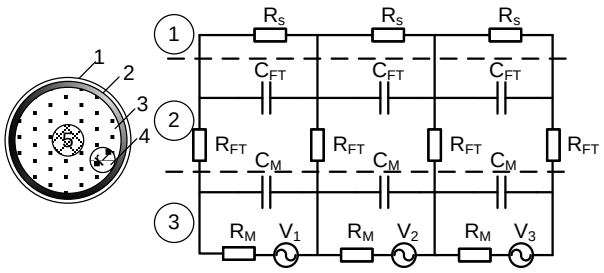

Fig. 2. Layer volume conduction model
1-Skin, 2 – Fat Tissue, 3 – Muscle Fiber, 4 – Motor Unit, 5 – Bone
r – radius of motor unit

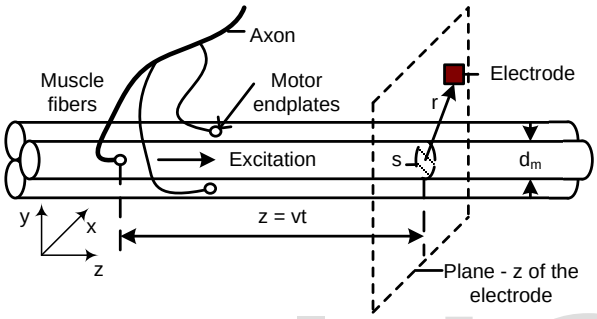

Fig. 3. A fiber action potential model

To illustrate the extracellular action potential which is obtained by using surface electrodes, a fiber action potential model is considered as presented in Fig. 3. The intracellular action potential, $V_F(z)$, in mV, is computed by (1)

$$V_F(z) = \begin{cases} 96(\lambda z)^3 \exp(-\lambda z) - 90, & if\ z > 0\ ; \\ 0, & otherwise \end{cases} \quad (1)$$

where, z, in mm, is the distance along the fiber and λ, in mm^{-1}, is a scale factor which can be defined by experiments [9]. By calculating the second derivative of $V_F(z)$, the equation of transmembrane current is yielded

$$I_F(z) = K_I \frac{d^2(V_F(z))}{dz^2} \quad (2)$$

where, K_I is a proportionality constant [9], [18]. To obtain results in time domain, z is substituted by $v.t$, where v is the propagation velocity of the action potential and t is the time value. According to E.V. Stalberg *et al* in [18], this velocity can be calculated by using the value of the fiber diameter d_m.

The single fiber action potential, $V_{AP}(z)$, in mm, can be yielded by (3)

$$V_{AP}(z) = K_V \int_S dS \int_{-\infty}^{+\infty} \frac{\partial V_F(z) \partial(1/r)}{\partial z^2} dz \quad (3)$$

where, K_V is a proportionality constant [19], and r is the distance between the fiber section S and the observation point [19]. Other papers calculated the above potential by using the convolution between the transmembrane current and the weighting function [9], [18]. The total of the single fiber action potentials is used to compute the motor unit action potential

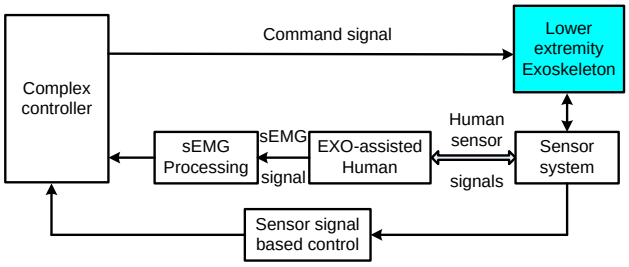

Fig. 4. A normal sEMG-based control scheme for a lower extremity exoskeleton system

$V_{MUAP}(t)$ which can be obtained by using surface electrodes. In order to create a real sEMG signal, $EMG(t)$, the additive noise, $n(t)$, is considered as given in (4)

$$EMG(t) = V_{MUAP}(t) + n(t) \quad (4)$$

where, $n(t)$ is chosen as a white noise for our work.

3 Processing Technique of sEMG Signal

The most important characteristic of sEMG signals is to reflect directly the human muscle activities [12]. As a result, they can be used to create main input signals such as force or torque to control a lower extremity exoskeleton robot in accordance with the user's motion intention. With their drawbacks as mentioned earlier, however, they have to be processed before using as input control signals.

Fig. 4 introduces a control scheme for a lower extremity exoskeleton robot. The signal processing block contains some steps which are used to process sEMG signal as expressed below:

(a) After acquisition, raw sEMG signals should be amplified with suitable gains.
(b) Amplified sEMG signals will be modified by using rectification or Root Mean Square (RMS) methods.
(c) Modified sEMG signals will be filtered by applying a FIR low pass filter with a 2-10 Hz cut-off frequency [17].

In the first step, to remove bias, it is necessary to calculate the mean of whole sEMG signals and then subtract it from each data point. In the second step, a full-wave rectification method is usually used to obtain the absolute values of sEMG signals. The other method which uses the definition of RMS is applied successfully in many researches [1], [12] because it gives a significant measure of the signal power.

In order to remove noises from sEMG signals to get the linear envelope of the signal as mentioned in the third step, a low pass filter can be used. In our work, to generate a good denoised sEMG signal, the continuous wavelet transform (CWT) will be used. The definition of CWT [3], [4] is expressed in (5)

$$CWT(a,b) = \frac{1}{\sqrt{a}} \int_{-\infty}^{+\infty} EMG(t).w\left(\frac{t-b}{a}\right) dt \quad (5)$$

where $EMG(t)$ is the analyzed signal, $w(t)$ is a mother wavelet function, b is a translation index, and a is scale parameter [5]. By applying CWT, noises in sEMG signal can be removed successfully because the signal energy only concentrates into few-

er coefficients while noise energy does not.

Though the amplitude of the processed sEMG signal at any instant in time is random, it is roughly proportional to the force exerted [1], [12], [21]. In this investigation, an EMG-to-force function is used to calculate corresponding force *F(A, B)* [21]

$$F(A,B) = A*[1-\exp(-B*EMG(t))] \quad (6)$$

where *EMG(t)* denotes the processed signal and *A*, *B* are two muscle parameters. These parameters belong to the type of muscle and they can be defined by experiments. For the calculation of sEMG-to-force, a normalization with the peak of *Maximum Voluntary Contraction* (MVC) is normally used [12], [14] to compare sEMG readings between subjects.

4 Simulation and Experiment Results

Although sEMG signals belong to many parameters, in our work, we only concentrate on simulation results in time domain concerning our experiment results. The intracellular action potential and the transmembrane current are plotted in Fig. 5(a) and Fig. 5(b), respectively. In Fig. 5(a), algebraic signs of the first derivative of *V(z)* affect the orientation of the dipoles: depolarization with the positive sign and repolarization with the negative sign. Fig. 5(b) expresses different shapes of the transmembrane current with different values of the fiber diameter: d_{min}, d_{max}, $d_{Tibialis\ Anterior}$, and $d_{Gastrocnemius\ Medialis}$. These values can be found well in [19]. To understand more clearly about the effect of the fiber diameter, Fig. 6 shows intracellular action potentials which belong to the change of this parameter. According to this relationship, minimum and maximum values of the intracellular action potential are shown stably, however, corresponding times are changeable.

To calculate the singly extracellular action potential, we can use either the definition of convolution or applying (3). Fig. 7 presents simulation results of an extracellular action potential by calculating the convolution of the transmembrane current and the weighting function. This weighting function is defined by J. Duchene *et al* in [9]. Algorithms of *Fast Fourier Transform* (FFT) and *Inverse Fast Fourier Transform* (IFFT) are also used to compute this extracellular action potential as signal train in Fig. 7(b).

By applying (4), sEMG signal and its PSD can be formed as presented in Fig. 8. Here, P.D.Welch's method is used to express the PSD of sEMG signal by using the corresponding function in MatLab software. This simulation result is similar in comparison with the Gaussian sEMG signal in Fig. 1. The shape of the simulated sEMG signal is clearly appropriate in accordance with the real signal.

In order to match with experiment results, three lower muscles of human leg are considered during the gait cycle. A human gait cycle is normally divided into two phases: stance phase and swing phase. These phases will be divided into seven smaller phases which can be found clearly in [22]. Three concerned human lower muscles are Gastrocnemius Medialis, Soleus, and Tibialis Anterior. The timing of the muscle activation and the intensity of muscle contraction in accordance with the different gait phases can be found in [19]. Simulation results of these lower muscles are shown in Fig. 9 during three human gait cycles. These simulation results have more significance to control our lower extremity exoskeleton which assists humans during normal walking with or without load carrying.

To apply a signal processing technique, the real sEMG signal of Gastrocnemius Medialis muscle is collected during a human gait cycle by our experiment. The raw sEMG signal in Fig. 10(a) will be processed by using *Signal Processing Toolbox* in Matlab software version 2011b. First, any DC offset will be removed from the raw sEMG signal, and then this signal is rectified by applying a full-wave rectification as shown in Fig. 10(b). Here, we can also use the RMS method to obtain absolute values of sEMG signal as plotted in Fig. 11(a). This absolute signal shape is similar to the rectified signal in Fig. 10(b). This rectified signal is then filtered by applying a low pass filter of a 10Hz cut-off frequency with the zero-phase digital filtering. Here, we also use the sampling frequency of 1000Hz and the 5th order filter. The filtered sEMG signal is shown in Fig. 11(b). In order to create the corresponding force, the EMG-to-force relationship in (6) is used. As a result, the obtained force in Fig. 11(c) can be used to generate the command signal as mentioned earlier in the control scheme for a lower extremity exoskeleton robot.

In this paper, the wavelet transform is also used to process sEMG signal by applying *Wavelet Toolbox Main Menu* in MatLab software. Normally, this technique can be used as a filter. For our work, it is applied to remove noises from modified sEMG signal after using RMS method. Result of this processing is expressed in Fig. 12. Wavelet function of Daubechies *db3, level 5* which has a matched shape with the motor action unit potential is used for our work. Fig. 13 shows more information of residuals for this processing, such as histogram, cumulative histogram, autocorrelations, and FFT-spectrum. According to these simulation results, most of the noises are removed effectively from sEMG signal to create the command signal more exactly.

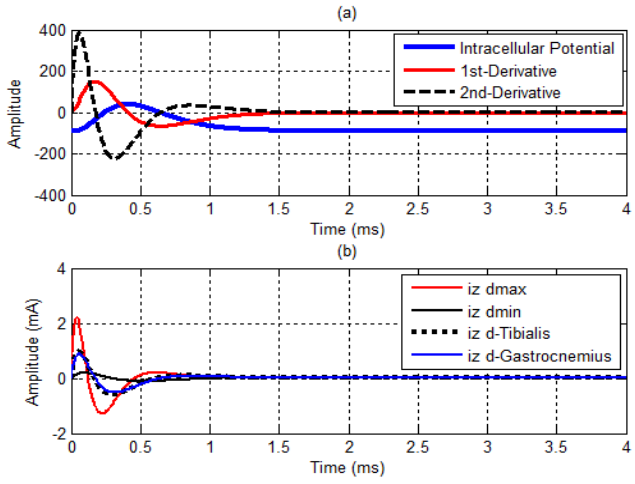

Fig. 5. The intracellular action potential and the transmembrane current
(a) The intracellular action potential and its derivatives
(b) The transmembrane current belongs to change of fober diameter: d_{min} = 25µm, d_{max} = 85 µm, $d_{Tibialis}$ = 57 µm and $d_{Gastrocnemius}$ = 54 µm.

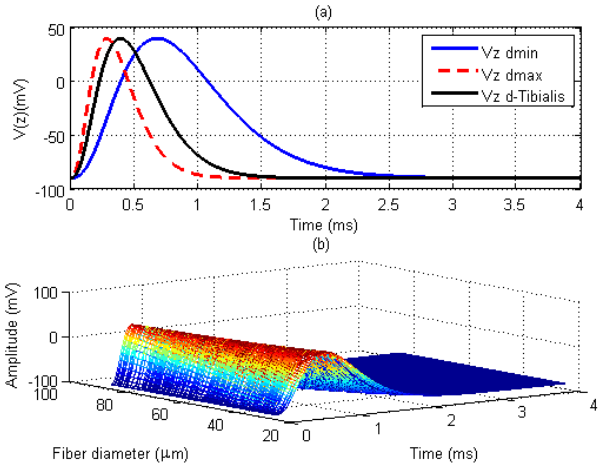

Fig. 6. The intracellular action potential belongs to the change of the fiber diameter.
(a) Intracellular action potentials of Tibialis anterior muscle, d_{min}, and d_{max}.
(b) Change of intracellular action potentials from d_{min} = 25µm, up to d_{max} = 85 µm.

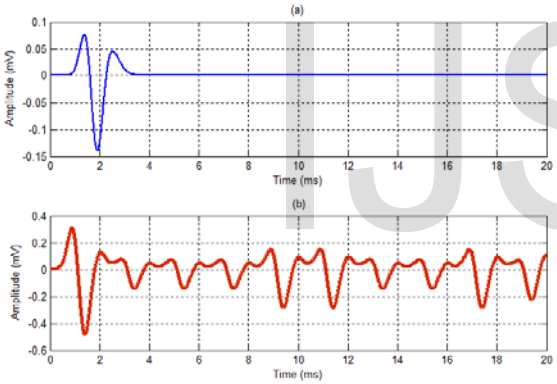

Fig. 7. A single fiber and motor unit action potential
(a) A single muscle fiber action potential which is calculated by the convolution of the transmembrane current and the weighting function.
(b) The motor unit action potential

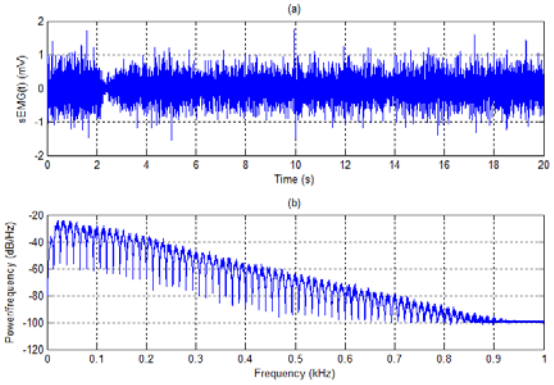

Fig. 8. Simulation of sEMG signal and its PSD
(a) sEMG signal with noises
(b) PSD of sEMG signal

4 Conclusion

This paper presents simulation and processing techniques of sEMG signal as the first part of our work in which a sEMG – based control scheme for a lower extremity exoskeleton robot has been designed successfully. Simulation results obtained play a significant role in accordance with our experiments, especially, in design of our system to assist soldiers who wear exoskeleton robots to work under hard conditions. By applying improved signal processing techniques, sEMG signal recording can be used efficiently to create the corresponding force which will be made the command signal for our exoskeleton system. For our work in the near future, we will develop strongly these techniques to design an exoskeleton – assisted system which can be applied widely in our real life.

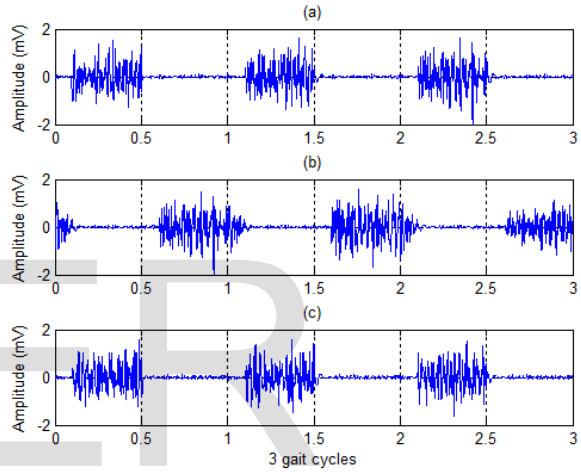

Fig. 9. Simulation of sEMG signal during 3 gait cycles
(a) Gastrocnemius Medialis
(b) Tibialis Anterior
(c) Soleus

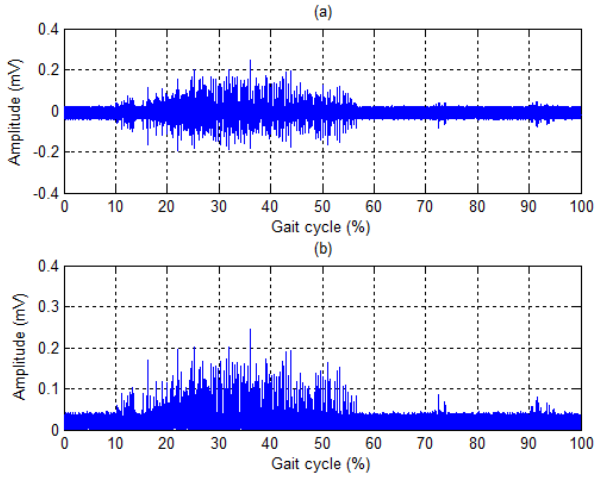

Fig. 10. Real sEMG signal from Gastrocnemius medialis during gait cycle
(a) Raw signal
(b) Rectified signal

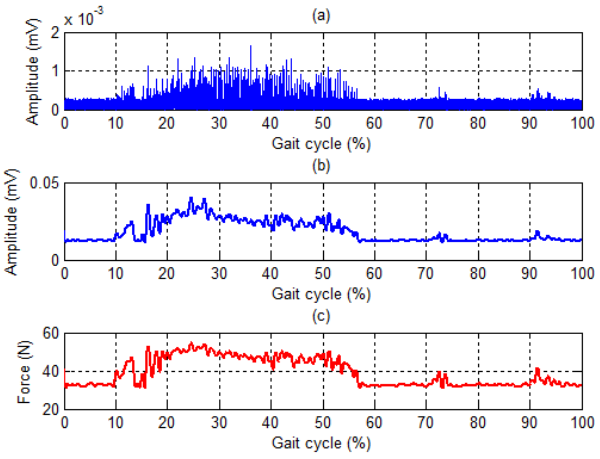

Fig. 11. The processed sEMG signal and the corresponding force
(a) RMS sEMG signal
(b) Filtered signal
(c) The corresponding force

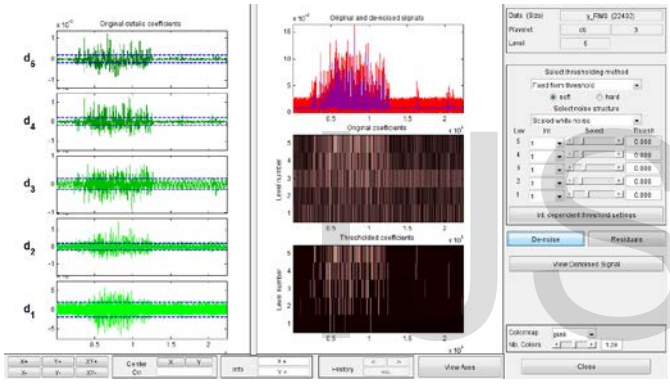

Fig. 12. De-noised sEMG signal by applying wavelet transform

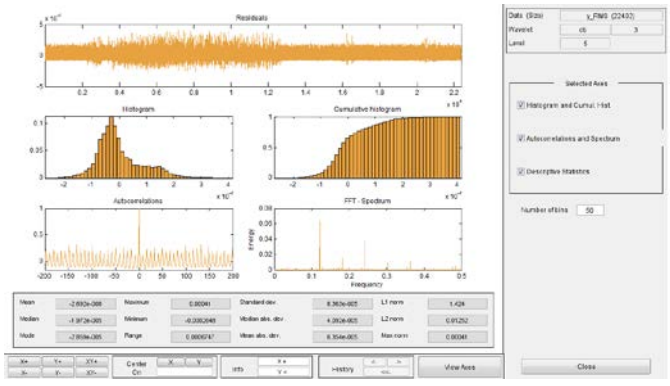

Fig. 13. More on residuals for wavelet transform to make the de-noised sEMG signal

ACKNOWLEDGMENT

The authors wish to thank members of PRMI laboratory for their support to perform this exoskeleton project.

REFERENCES

[1] Christian Fleicher, Konstantin Kondak, Christian Renicke, and Guiter Hommel, "Online Calibration of the EMG to Force Relationship", *Proc. IEEE/RSJ. International Conference on Intelligent Robots and Systems*, pp. 1305-1310, Sept. 28 - Oct. 2, 2004.

[2] Claudia U. Ranniger and David L. Akin, "EMG Mean Power Frequency Determination Using Wavelet Analysis," *Proc. IEEE/EMBS. 19th International Conference*, pp. 1589-1592, Oct. 30- Nov. 2, 1997.

[3] Ali N. Akansu, Wouter A.Serdijin, and Ivan W. Selesnick, "Emerging Applications of Wavelets: A Review", *Physical Communication*, pp. 1-18, 2010.

[4] Oliver Rioul and Martin Vetteru, "Wavelets and Signal Processing," *IEEE SP Magazine*, pp. 14-35, Oct. 1991.

[5] Qi Xu, Yazhi Quan, Lei Yang, and Jiping He, "An Adaptive Algorithm for the Determination of the Onset and Offset of Muscle Contraction by EMG Signal Processing," *IEEE Trans. Neural Systems and Rehabilitation Engineering*, vol. 21, no. 1, pp. 65-73, Jan. 2013.

[6] A.K. Mahabalagini, K. Ahmed and F.Schlereth, "A Novel Approach for Simulation, Measurement and Representation of Surface EMG Signals", *Conference Record of the Forty Fifth Asilomar Conference on.* ASILOMAR 2011: Signals, Systems and Computers, pp. 476-480, 2011.

[7] Ram Murat Singh and S. Chatterji, "Trends and Challenges in EMG Based Control Scheme of Exoskeleton Robots - A Review." *International Journal of Scientific and Engineering Research*, vol. 3, no.8, pp. 1-8, 2012.

[8] Gregory S. Sawicki and Daniel P. Ferris, "Mechanics and Energetics of Incline Walking with Robotic Ankle Exoskeletons", *Journal of Experimental Biology*, vol. 212, no.1,pp. 32-41, 2009.

[9] J. Duchene and J.-Y. Hogrel, "A Model of EMG Generation", *IEEE Trans. Biomedical Engineering*, vol. 47, no.2, pp. 192-201, 2000.

[10] Kazuo Kiguchi and Y. Imada, "EMG-based Control for Lower-Limb Power-Assist Exoskeletons", *IEEE Workshop on.* RIISS '09: Robotic Intelligence in Informationally Structured Space, pp. 19-24, 2009.

[11] H.He and K. Kiguchi, "A Study on EMG-based Control of Exoskeleton Robots for Human Lower-Limb Motion Assist", *6th International Special Topic Conference on.* ITAB 2007: Information Technology Application in Biomedicine, pp. 292-295, 2007.

[12] Konral, Peter, *The ABC of EMG,* A Practical Introduction to Kinesiological Electromyography, pp.30-55, 2005.

[13] Fansan Zhu and N. W. Levin, "An Electrical Resistivity Model of Segmental Body Composition Using Bioimpedance Analysis", *Proceedings of the 25th Annual International Conference of the IEEE.* Engineering in Medicine and Biology Society, pp. 2679-2682, 2003.

[14] D.P. Ferris and C.L. Lewis, "Robotic Lower Limb Exoskeleton Using Proportional Myoelectric Control", *Annual International Conference of the IEEE.* Engineering in Medicine and Biology Society, pp. 2119-2124, 2009.

[15] Dario Farina and Roberto. Merletti, "A Novel Approach for Precise Simulation of the EMG Signal Detected by Surface Electrodes", *IEEE Trans. Biomedical Engineering*, pp. 637-646, 2001.

[16] O. Unluhisarcikli, M. Pietrusinski, B. Weinberg, P. Bonato, and C. Mavroidis, "Design and Control of a Robotic Lower Extremity Exoskeleton for Gait Rehabilitation", *2011 IEEE/RSJ International Conference on.* Intelligent Robots and Systems (IROS), pp. 4893-4898, 2011.

[17] S. Patrick, J. Meklenburg, S. Jung, Y. Mendelson, and E.A. Clancy, "An Electromyogram Simulator for Myoelectric Prosthesis Testing", *Proceedings of the 2010 IEEE 36th Annual Northeast.* Bioengineering Conference,pp. 237-243, 2010.

[18] Sanjeev D.Nandedkar, E.V. Stalberg and Donald B.Sanders, "Simulation Techiques in Electromyography", *IEEE Trans. Biomedical Engineering,* vol. 32, no. 10, pp. 775-785, 1985.

[19] W. Wang, A. De. Stefano, and R.Allen, "A Simulation Model of the Surface EMG Signal for Analysis of Muscle Activity During the Gait Cycle", *Computer in Biology and Medicine,* vol. 36, no. 6, pp. 601-618, 2006.

[20] A. Salman, J. Iqbal, U. Izhar, U.S. Khan, and N. Rashid, "Optimized Circuit for EMG Signal Processing", *2012 International Conference on.* Robotics and Artificial Intelligence (ICRAI), pp. 208-213, 2012.

[21] Mitsuhiro Hayashibe, David Guiraud, and Philippe Poignet, "EMG-to-Force Estimation with Full-Scale Physiology Based Muscle Model", *Proc. IEEE/RSJ. International Conference on Intelligent Robots and Systems*, pp. 1621-1626, Oct. 11-15, 2009.

[22] Chetas D. Joshi, Uttama Lahiri, and Nitish V. Thakor, "Classification of Gait Phases from Lower Limb EMG: Application to Exoskeleton Orthotics," *2013 IEEE Point-of-Care Healthcare Technologies*, pp. 228-231, Jan. 2013.